



## Characterization of nanoscale zero valent iron modified by nonionic surfactant for trichloroethylene removal in the presence of humic acid: A research note

Young-Chul Lee<sup>a</sup>, Chul-Woong Kim<sup>a</sup>, Jae-Young Lee<sup>b</sup>, Hyun-Jae Shin<sup>c</sup>, Ji-Won Yang<sup>a\*</sup>

<sup>a</sup>Laboratory of Nano Environmental Engineering, Department of Chemical and Biomolecular Engineering (BK 21 Program), KAIST, 335 Gwahangno, Yuseong-gu, Daejeon 305-701, Korea

Tel. +82 (42) 350-3924; Fax +82 (42)350-3910; email: jwyang@kaist.ac.kr

<sup>b</sup>Railroad Environment Research Department, Korea Railroad Research Institute (KRRRI) 360-1, Woram-dong, Uiwang-si, Gyeonggi-do 437-757, Korea

<sup>c</sup>Department of Chemical & Biochemical Engineering, Chosun University, Seosuk-dong, Dong-gu, Gwangju 501-759, Korea

Received 29 August 2008; accepted in revised form 26 June 2009

### ABSTRACT

Trichloroethylene (TCE) is a common contaminant in water and groundwater, known as suspected carcinogens, and its presence in the environment is of significant concern. Nano-scale zero-valent iron (NZVI) has emerged as an excellent reduction catalyst due to fast degradation of chlorinated solvents. However aggregation of NZVI is a serious limitation. In this study, NZVI was coated with nonionic surfactant to overcome its aggregation and to enhance its dispersion. The synthesized NZVI using water-based solution method produced nanowire-like structures mostly and a few portion of NZVI showed a spherical shape. For the modification of NZVI by surfactant, the amount of Tween 80<sup>®</sup> used to be adsorbed onto NZVI was ca. 8 mmol/kg of NZVI. The volume size distribution of the obtained surfactant modified NZVI (SNZVI) increased to  $d_{90\%}$  (cumulative size at 90%) = 2.03  $\mu\text{m}$  and at 0.79  $\mu\text{m}$  of mean size, while that of bare NZVI had diameter with  $d_{90\%}$  (cumulative size at 90%) = 14.12  $\mu\text{m}$  and at 4.54  $\mu\text{m}$  of mean size. The maximum adsorption amount of humic acid (HA) onto SNZVI was 18.70 mg/g and that of NZVI was 20.05 mg/g. For TCE removal in the presence of HA, SNZVI was not enhanced for TCE removal efficiency, compared with NZVI removal. And TCE removal using SNZVI was inhibited as HA concentration increased, but TCE degradation efficiency increased at high concentration of HA. Based on reduction of size and the reactivity of SNZVI, the present results can be applied for in situ groundwater remediation.

*Keywords:* Nanoscale zero valent iron; Trichloroethylene; Nonionic surfactant; Humic acid

### 1. Introduction

Human health has been threatened in water and groundwater contaminated by chlorinated compounds such as trichloroethylene (TCE), perchloroethylene (PCE) with a potential to suspect carcinogens [1,2]. For the remediation of groundwater contaminated with chlorinated

contaminants, microscale zero valent iron ( $\mu\text{ZVI}$ ) has been investigated to dechlorinate chlorinated compounds. In case of  $\mu\text{ZVI}$ , many researches had focused on the enhancement of reaction rate by modifying with surfactants and had observed the effect of natural organic matter (NOM) of ubiquitous existence in water and groundwater during carbon tetrachloride (CT) and TCE reaction [3–7].

Since the beginning of 2000, nanoscale zero valent iron (NZVI) has issued as an excellent catalyst for redox

\* Corresponding author.

reaction and Fenton process due to a large surface area, a higher reactivity, nontoxicity, and inexpensiveness in environmental remedy [8–14].

Despite a large surface area of NZVI, these nanoparticles have limitations such as its aggregation and agglomeration, which is difficult to transport into porous media in target contaminated sites [15]. Therefore, hydrophilic carbon, polyacrylic acid and cellulose coated with NZVI were tested for the transport in soil and groundwater and were applied to remove arsenic and chromate [16–21]. Another NZVI modification method was to use cationic and nonionic surfactants to increase in its surface area and dispersion. In this study, nonionic surfactant with a higher HLB value was selected to modify NZVI for a stable dispersion in water solution. Generally, cationic surfactants was known as a toxic material among types of surfactants and adsorbed onto negative charged soil surfaces easily, while anionic surfactant had a low reduction rate [5,22]. From these characteristics, cationic and anionic surfactants were not suitable as an agent for the modification of NZVI. The objective of the present research was to investigate TCE removal by surfactant modified NZVI (SNZVI) in the presence of HA. The specific studies of these works were as follows: (1) selection of NZVI precursors as an electron donor, (2) preparation and characterization of SNZVI, (3) investigation of the effect of HA concentration for TCE removal using SNZVI.

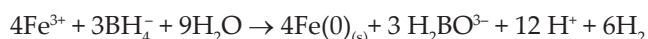
## 2. Experimental

### 2.1. Chemicals

All chemicals of iron(III) chloride hexahydrate (97%, ACS reagent), sodium borohydride ( $\geq 98.5\%$ , reagent grade), trichloroethylene (99.5+%, ACS reagent), Tween<sup>®</sup>80 and humic acid (sodium salt) were obtained from Sigma-Aldrich.

### 2.2. Preparation of SNZVI

Zero valent iron nanoparticulates were collected by dropping 1:1 volume ratio of  $\text{NaBH}_4$  (0.25 M) into  $\text{FeCl}_3 \cdot 6\text{H}_2\text{O}$  (0.05 M) solution [11]. The reduction reaction of ferric ions with borohydride is as follows:



1 g of the synthesized NZVI was put into  $\text{N}_2$  purged of 10 mM Tween<sup>®</sup> 80 solution in 60 ml bottle and was mixed continuously in end-over-end shaker during the night. Black precipitates were separated by centrifugation, washed twice with deionized water and then dried in a vacuum oven for 1 day.

### 2.3. TCE removal with SNZVI

2 mg of SNZVI was put into vials and injected with 20 ml of initial  $29.26\text{ mgL}^{-1}$  TCE solution. And then im-

mediately vortexed them at 5 s, 10 s, 20 s, and 30 s, and these samples were filtered and analyzed. In case of above 30 s reaction time, all samples were stirred by end-over shaker for specified time intervals immediately after 30 s vortexing. All experiments were performed in triplicate.

To confirm of TCE degradation, chloride ion was measured with ion chromatograph (IC-Pak anion HR column, Water 432 conductivity detector) in both NZVI and SNZVI without HA, whose detection limit is  $0.1\text{ mgL}^{-1}$ .

### 2.4. Characterization and analysis

Surface morphology for NZVI was observed with FE-TEM (model, JEM-2100F HR, 200 kV) and FE-SEM (Sirion, FEI). The distribution of particle size was analyzed by a particle size analyzer (Beckman coulter LS230, Brea, USA).  $\text{N}_2$  sorption/desorption data were obtained using a gas sorption analyzer (NOVA 4200 Ver. 7.10). The specific surface area was calculated by the BET equation. X-ray diffraction (XRD) data were obtained on a Rigaku D/max IIIc (3 kW) with a  $\theta/\theta$  goniometer equipped with a  $\text{CuK}\alpha$  radiation generator at 40 kV and 45 mA and the scan range was from 10 to  $70^\circ$  (or  $80^\circ$ )  $2\theta$  at a rate of  $3^\circ$  (or  $1.2^\circ$ )  $2\theta/\text{min}$ .

Tween 80<sup>®</sup> and HA concentration were measured with UV-Vis spectroscopy (Hewlett Packard 8452A, USA) at a wavelength of 230 nm, and 254 nm respectively [22]. HPLC (high performance liquid chromatograph) was used to analyze TCE concentration. The HPLC was operated at a wavelength of 214 nm. Elution was performed with acetonitrile/water (80/20, v/v) at a flow rate of 1.0 ml/min.

## 3. Results and discussion

### 3.1. Characteristics of iron nanoparticles by different precursors

TEM image of iron nanoparticles (NZVI) synthesized by chloride precursor showed numerous nanowire structures, diameters ranging ca. 20–120 nm, while iron nanoparticles by nitrate precursor reveals the diameter of particles, ca. 2–6 nm with individual fiber structures (data not shown). The average diameter of iron nanoparticles by nitrate precursor (mean 126 nm) is less than the one by chloride precursor (182 nm) (Table 1). This result suggests that the particles are easily aggregated and do not exist in individual forms due to spontaneous aggregation of nanoparticles [16]. The XRD pattern (Fig. 1) of NZVI by chloride iron precursor matched well with cubic Fe (0) standard patterns without iron oxide peaks. Sometimes iron oxide peaks appeared with synthesis condition [11,25]. However, the XRD pattern (Fig. 1) of iron nanoparticles by nitrate iron precursor indicates amorphous iron (III) state. Therefore we concluded that NZVI by chloride precursor is a proper candidate as an electron donor to transformation of TCE to nontoxic products.

Table 1

The number particle size and its distribution of iron nanoparticles by  $\text{Cl}^-$  and  $\text{NO}_3^-$  NZVI precursor (above two lines), the volume particle size and its distribution of NZVI and SNZVI (below two lines)

	$d_{10\%}$ ( $\mu\text{m}$ )	$d_{50\%}$ ( $\mu\text{m}$ )	$d_{90\%}$ ( $\mu\text{m}$ )	Mean	SD
$\text{Cl}^-$ - NZVI	0.08	0.17	0.30	0.18	0.11
$\text{NO}_3^-$ - NZVI	0.06	0.09	0.18	0.13	0.28
NZVI	0.23	2.62	14.12	4.54	5.32
SNZVI	0.18	0.38	2.03	0.79	0.76

Note:  $d_{10\%}$ ,  $d_{50\%}$ , and  $d_{90\%}$  are the cumulative probability sizes at 10 %, 50 %, and 90%

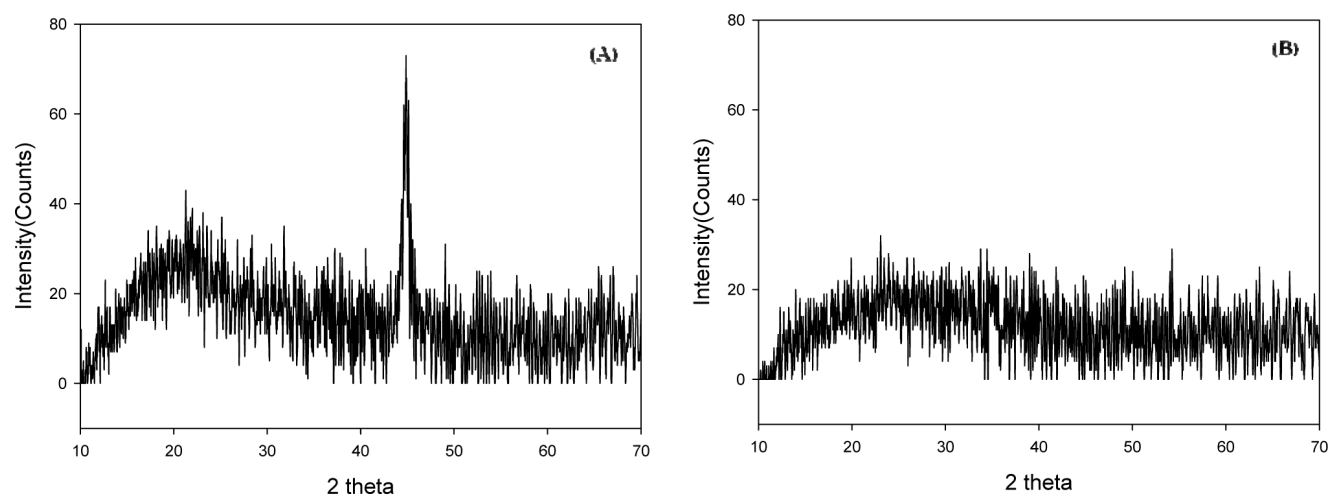


Fig. 1. XRD pattern of iron nanoparticles (A)  $\text{Cl}^-$  and (B)  $\text{NO}_3^-$  precursors

### 3.2. Characteristics of NZVI and SNZVI

Particle size distribution (PSD) of NZVI (chloride iron precursor reduction) and SNZVI were summarized in Table 1. The NZVI had a median size of  $2.62 \mu\text{m}$  and a mean size of  $4.54 \mu\text{m}$ , distributing within maximum ca.  $27.5 \mu\text{m}$  of diameter. On the other hand, SNZVI had a median size of  $0.38 \mu\text{m}$  and a mean size of  $0.80 \mu\text{m}$ , distributing within maximum ca.  $3 \mu\text{m}$  diameters. Even though the number size distribution of NZVI and SNZVI was slightly different (data not shown), their volume size distribution indicated a significant size reduction in SNZVI, resulting in the decrease of about one order magnitude (NZVI  $< 27.5 \mu\text{m}$ , SNZVI  $< 3 \mu\text{m}$ ). In addition, BET surface area of NZVI was  $25.01 \text{ m}^2/\text{g}$  and that of SNZVI was  $37.07 \text{ m}^2/\text{g}$ . This value of NZVI is less than the previous result reported in literature, whose surface area of NZVI was ca.  $33.5 \text{ m}^2/\text{g}$  [8,15]. However, a surface area of NZVI was ranged with  $10\text{--}40 \text{ m}^2/\text{g}$ , depending on synthesis condition of NZVI [8,25].

### 3.3. TEM and SEM analysis of SNZVI and HA adsorbed onto SNZVI

Fig. 2 shows the images by TEM and SEM of SNZVI and the HA adsorbed SNZVI. The diameter of aggregates in chains of NZVI was  $34\text{--}140 \text{ nm}$  (Figs. 2A and 2B), which corresponded with diameter  $40\text{--}120 \text{ nm}$  of SEM image (Fig. 2C). Inset of Fig. 2a was selected area electron ring diffraction, revealing polycrystalline structure. In the case of SEM image of HA adsorbed onto SNZVI, Fig. 2D shows a rough and plate-like structure, which was a little different morphology.

### 3.4. XRD measurement before/after TCE reaction

Based on XRD data, the sharp peak of Fe (0) disappeared and was changed to iron oxide ( $\gamma\text{-Fe}_2\text{O}_3$ ) after TCE reaction with NZVI and SNZVI (Fig. 3), which showed that reduction potential of NZVI was almost lost. Comparing with NZVI and SNZVI in deionized water, NZVI was maintained Fe(0) peak and appeared the weak iron



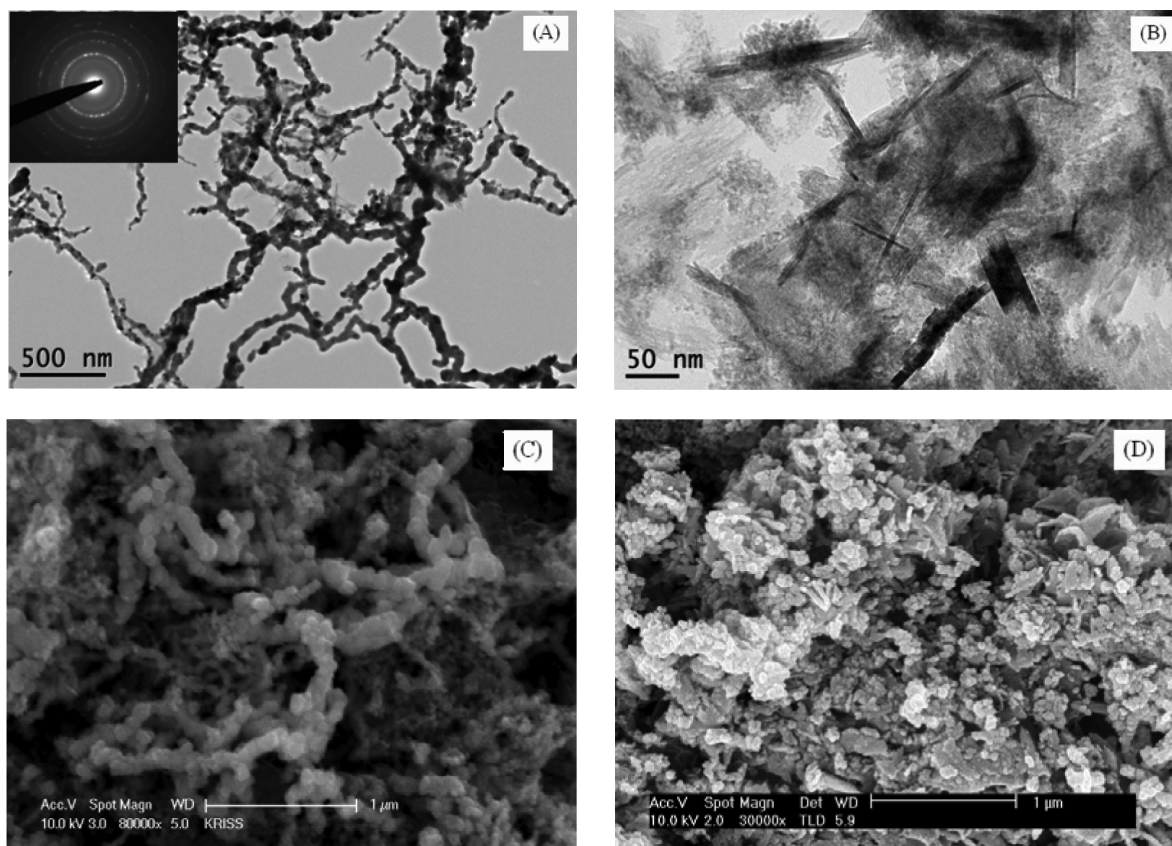


Fig. 2. TEM image (A) and high resolution TEM images (B) of SNZVI, inset of (A): Selected area electron ring diffraction, SEM image (C) of SNZVI and (D) of HA adsorbed SNZVI.

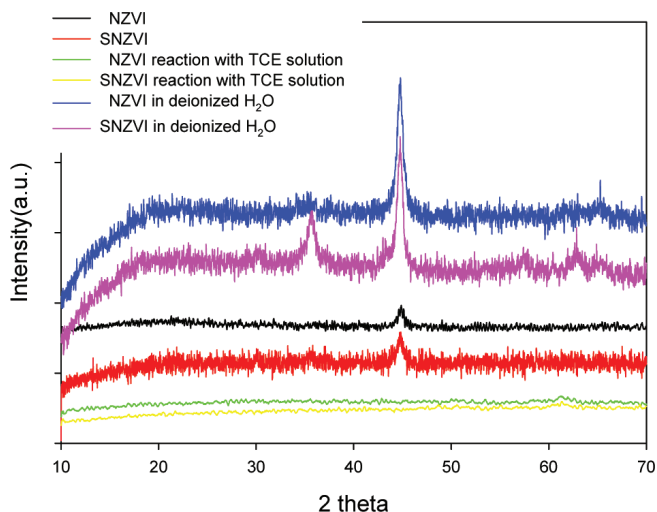


Fig. 3. XRD pattern of NZVI and SNZVI before/after TCE reaction, NZVI and SNZVI in deionized H<sub>2</sub>O was measured at a rate of 1.2° 2θ/min to see detailed effect of oxidation, others were measured at a rate of 3° 2θ/min.

oxide ( $\gamma\text{-Fe}_2\text{O}_3$ ) peak, and also SNZVI showed similar pattern except distinct iron oxide ( $\gamma\text{-Fe}_2\text{O}_3$ ) peak at ca.

$2\theta = 35$ . Therefore because both NZVI and SNZVI in water showed iron oxide even though main Fe (0) peak was retained, reduction of reactivity and control of NZVI and SNZVI oxidation for TCE might be important for environmental remediation.

### 3.5. HA adsorption onto NZVI and SNZVI

Fig. 4 illustrates the adsorption isotherm of NZVI (A) and SNZVI (B), respectively. Both NZVI and SNZVI were adsorbed within ca. 20 min (data not shown). In Fig. 4, adsorption isotherms of NZVI and SNZVI presented an S-type isotherm, in which the slope initially increased with adsorptive concentration, but eventually decreased and became a saturated plateau [24]. The  $q$  value of NZVI was ca. 20.05 mg/g while that of SNZVI was 18.70 mg/g, these values were the results from the competitive adsorption between surfactant and HA on the surface of NZVI [5,22].

### 3.6. Effect of HA for TCE removal using SNZVI

A hydrophobic TCE was moved onto the surface of NZVI through the admicelle and the monomers of surfactant onto NZVI [3,6]. Adsorption of TCE by SNZVI was so fast that TCE was removed from initial 29.26 mg/L to

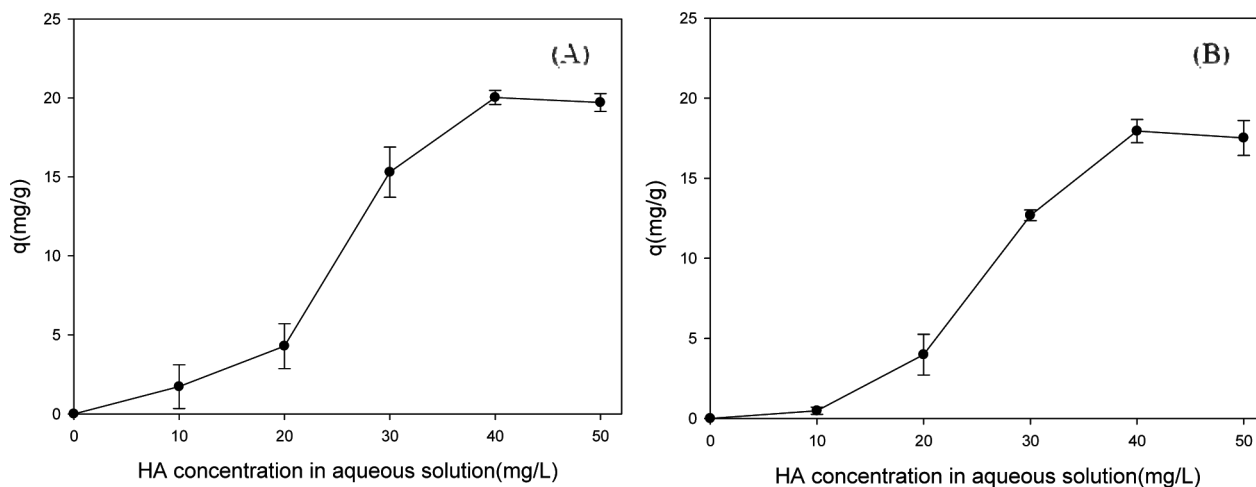


Fig. 4. HA adsorption onto NZVI (A) and SNZVI (B).

almost 3 mg/L during 30 s of vortexing, and the removal ability of SNZVI decreased sharply whose removal were sorption and degradation due to the detection of less concentration of chloride ions, based on theoretically, produced chloride ions during TCE removal (Fig. 5). Nonionic surfactant monomers coated on the surface of NZVI, which improved not only mass-transport between NZVI and TCE molecules but also the size distribution of NZVI, however, did not decrease the TCE removal significantly. If we consider increase in the surface area of SNZVI, surfactants competitively occupied the reactive sites of NZVI surface with TCE. Even though SNZVI enhanced transportability for porous media, but the removal, especially degradation effect was not improved when considering the measured chloride ions (Fig. 5B). In addition, as HA concentration increased, TCE removal was decreased [6]. However, TCE degradation rather in-

creased slightly at a higher concentration of HA (50 mg/L) because of the effect of electron shuttle [5,23].

#### 4. Conclusions

The NZVI synthesized by chloride iron precursor in this study was an appropriate nanoparticle for TCE removal. The size distribution of NZVI decreased an order of magnitude by modifying with nonionic surfactant. TCE removal using SNZVI was inhibited as HA concentration increased, while its rate remained still fast at the initial time. HA was functioned competitively with TCE onto the surface of SNZVI. As a result, TCE removal decreased while the quinone compounds in HA enhanced TCE dechlorination rate by SNZVI at higher HA. However electron shuttle effect is not important for *in-situ* remediation due to a low concentration of HA in the nature

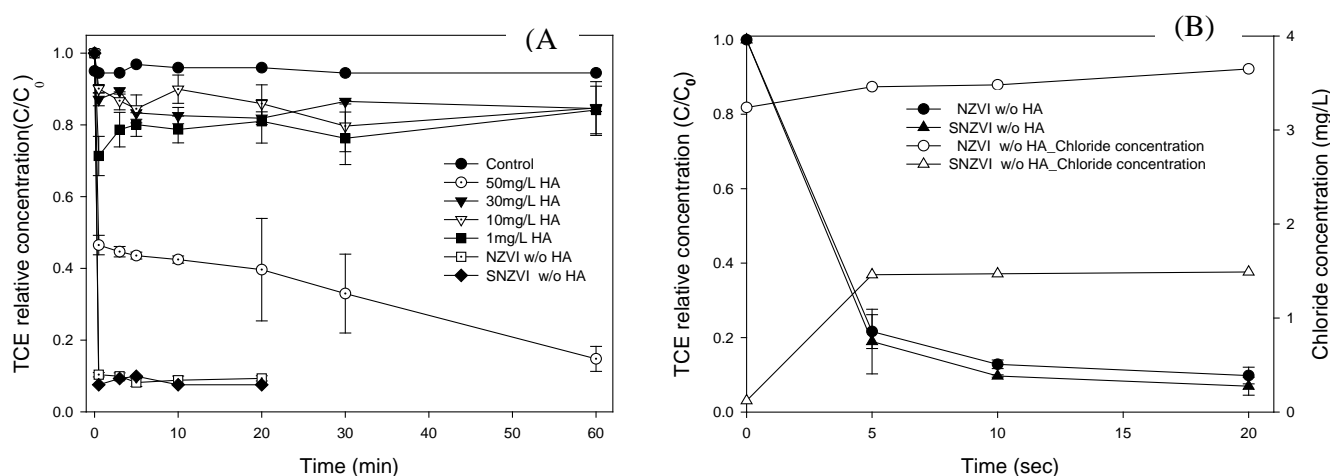


Fig. 5. TCE removal using SNZVI according to HA concentration (A) and initial TCE removal rate of NZVI and SNZVI and concentration of chloride ions (B).

environment (< 1mg/L). As the HA accumulated onto SNZVI for a long time, TCE degradation would be improved [26]. In conclusion, due to a significant reduction in size, SNZVI can apply TCE contaminated sites, maintaining a comparable reactivity as much as pristine NZVI.

### Acknowledgements

This research was supported by Korean Ministry of Environment as “The GAIA Project”. We thanks all members of National NanoFab Center (NNFC) for fruitful discussions about TEM and SEM imaging.

### References

- [1] J.F. Pankow and J.A. Cherry, Dense chlorinated solvents, Waterloo Press, Portland, 1996.
- [2] Y.C. Lee, T.S. Kwon, J.S. Yang and J.W. Yang, Remediation of groundwater contaminated with DNAPLs by biodegradable oil emulsion, *J. Hazard. Mater.*, 140 (2007) 340.
- [3] Z. Li, Degradation of perchloroethylene by zero valent iron modified with cationic surfactant, *Adv. Environ. Res.*, 2 (1998) 244.
- [4] Z. Li, C. Willms, J. Alley, P. Zhang and R.S. Bowman, A shift in pathway of iron-mediated perchloroethylene reduction in the presence of sorbed surfactant – A column study, *Water Res.*, 40 (2006) 3811.
- [5] P.G. Tratnyek, M.M. Scherer, B. Deng and S. Hu, Effects of natural organic matter, anthropogenic surfactants, and model quinones on the reduction of contaminants by zero-valent iron, *Wat. Res.*, 35 (2001) 4435.
- [6] H.H. Cho and J.W. Park, Sorption and reduction of tetrachloroethylene with zero valent iron and amphiphilic molecules, *Chemosphere*, 64 (2006) 1047.
- [7] M.C. Shin, H.D. Choi, D.H. Kim and K. Baek, Effect of surfactant on reductive dechlorination of trichloroethylene by zero-valent iron, *Desalination*, 223 (2008) 299.
- [8] L. Li, M. Fan, R.C. Brown, J.V. Leeuwen, J. Wang, W. Wang, Y. Song and P. Zhang, Synthesis, properties, and environmental applications of nanoscale iron-based materials: A review, *Cri. Rev. Env. Sci. Tec.*, 36 (2006) 405.
- [9] L. Machala, R. Zboril and A. Gedanken, Amorphous iron (III) oxide: A review, *J. Phys. Chem. B*, 111 (2007) 4003.
- [10] C.J. Liao, T.L. Chung, W.L. Chen and S.L. Kuo, Treatment of pentachlorophenol-contaminated soil using nano-scale zero-valent iron with hydrogen peroxide, *J. Mol. Catal. A-Chem.*, 265 (2007) 189.
- [11] H.L. Lien and W.X. Zhang, Nanoscale Pd/Fe bimetallic particles: Catalytic effects of palladium on hydrodechlorination, *Appl. Catal. B-Environ.*, 77 (2007) 110.
- [12] S.H. Joo, A.J. Feitz and T.D. Waite, Oxidative degradation of the carbothioate herbicide, molinate, using nanoscale zero-valent iron, *Environ. Sci. Technol.*, 38 (2004) 2242.
- [13] A.J. Feitz, S.H. Joo, J. Guan, Q. Sun, D.L. Sedlak and T.D. Waite, Oxidative transformation of contaminants using colloidal zero-valent iron, *Colloid Surface A*, 265 (2005) 88.
- [14] A. Ghauch, Rapid removal of flutriafol in water by zero-valent iron powder, *Chemosphere*, 71 (2008) 816.
- [15] W. Zhang, Nanoscale iron particles for environmental remediation: A review, *J. Nanopart. Res.*, 5 (2003) 323.
- [16] Y. Xu and D. Zhao, Reductive immobilization of chromate in water and soil using stabilized iron nanoparticles, *Water Res.*, 41 (2007) 2101.
- [17] B. Shrick, B.W. Hydutsky, J.L. Blough and T.E. Mallouk, Delivery vehicles for zerovalent metal nanoparticles in soil and groundwater, *Chem. Mater.*, 16 (2004) 2187.
- [18] Y.P. Sun, X.Q. Li, W. X. Zhang and H.P. Wang, A method for the preparation of stable dispersion of zero-valent iron nanoparticles, *Colloid Surface A*, 308 (2007) 60.
- [19] Z. Xiong, D. Zhao and G. Pan, Rapid and complete destruction of perchlorate in water and ion-exchange brine using stabilized zero-valent iron nanoparticles, *Water Res.*, 41 (2007) 3497.
- [20] S.R. Kanel, D. Nepal, B. Manning and H. Choi, Transport of surface-modified iron nanoparticle in porous media and application to arsenic (III) remediation, *J. Nanopart. Res.*, 9 (2007) 725.
- [21] S.R. Kanel and H. Choi., Transport characteristics of surface-modified nanoscale zero-valent iron in porous media, *Water Sci. Technol.*, 55 (2007) 157.
- [22] A.M. Giasuddin, S.R. Kanel and H. Choi., Adsorption of humic acid onto nanoscale zerovalent iron and its effect on arsenic removal, *Environ. Sci. Technol.*, 41 (2007) 2022.
- [23] R.A. Doong and T.J. Lai, Dechlorination of tetrachloroethylene by palladized iron in the presence of humic acid, *Water Res.*, 39 (2005) 2309.
- [24] D.L. Sparks, *Environmental Soil Chemistry*, Academic Press, 1995.
- [25] Z. Ai, L. Lu, J. Li, L. Zhang, J. Qiu and M. Wu, Fe@Fe<sub>2</sub>O<sub>3</sub> core-shell nanowires as iron reagent. 1. Efficient degradation of Rhodamine B by a novel sono-Fenton process, *J. Phys. Chem. C*, 111 (2007) 4087.
- [26] A. Georgi, A. Schierz, U. Trommler, C.P. Horwitz, T.J. Collins and F.D. Kopinke, Humic acid modified Fenton reagent for enhancement of the working pH range, *Appl. Catal. B-Environ.*, 72 (2007) 26.